SUPPORTING INFORMATION

Response of a Macrotidal Estuary to Changes in Anthropogenic Mercury Loading between 1850 and 2000

Elsie M. Sunderland[†*], *John Dalziel*[‡], *Andrew Heyes*[§], *Brian A. Branfireun*[||], *David P. Krabbenhoft*[⊥], *Frank A.P.C. Gobas*[⌠]

[†]Harvard University, School of Engineering and Applied Sciences, Cambridge MA, 02138, USA

[‡]Environment Canada, Meteorological Service of Canada, 45 Alderney Drive, Dartmouth, Nova Scotia, B2Y 2N6, Canada

[§]Chesapeake Biological Laboratory, University of Maryland Center for Environmental Science, University System of Maryland, Solomons, MD, 20688, USA

[||]Department of Geography, University of Toronto at Mississauga, 3359 Mississauga Road North, Mississauga, Ontario, L5L 1C6, Canada

[⊥]U.S. Geological Survey, 8505 Research Way, Middleton, WI, 53562, USA

[⌠]School of Resource and Environmental Management, Simon Fraser University, Burnaby, British Columbia, V5A 1S6, Canada

Contents **Page(s)**

Figure S1	Conceptual overview of model	2
Figure S2/Table S1	Supplemental sensitivity analysis results	3
Section I	Site-specific data	4-6
Section II	Model differential equations	7-8
Section III	External loading	9-10
Section IV	Derivation of model rate coefficients	11-17
	References	18-20

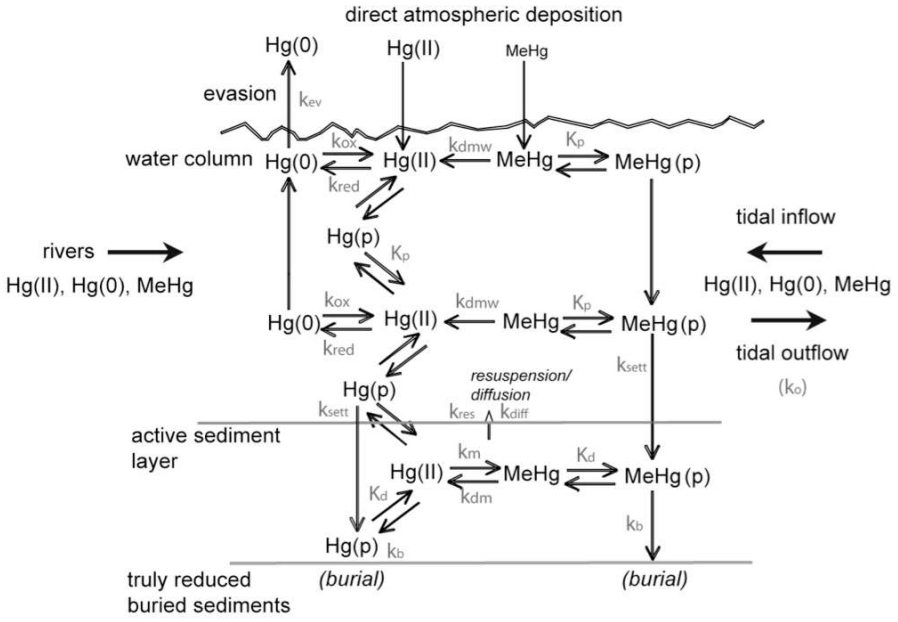

Figure S1. Conceptual diagram of Hg transport and transformation processes included in estuarine Hg cycling model.

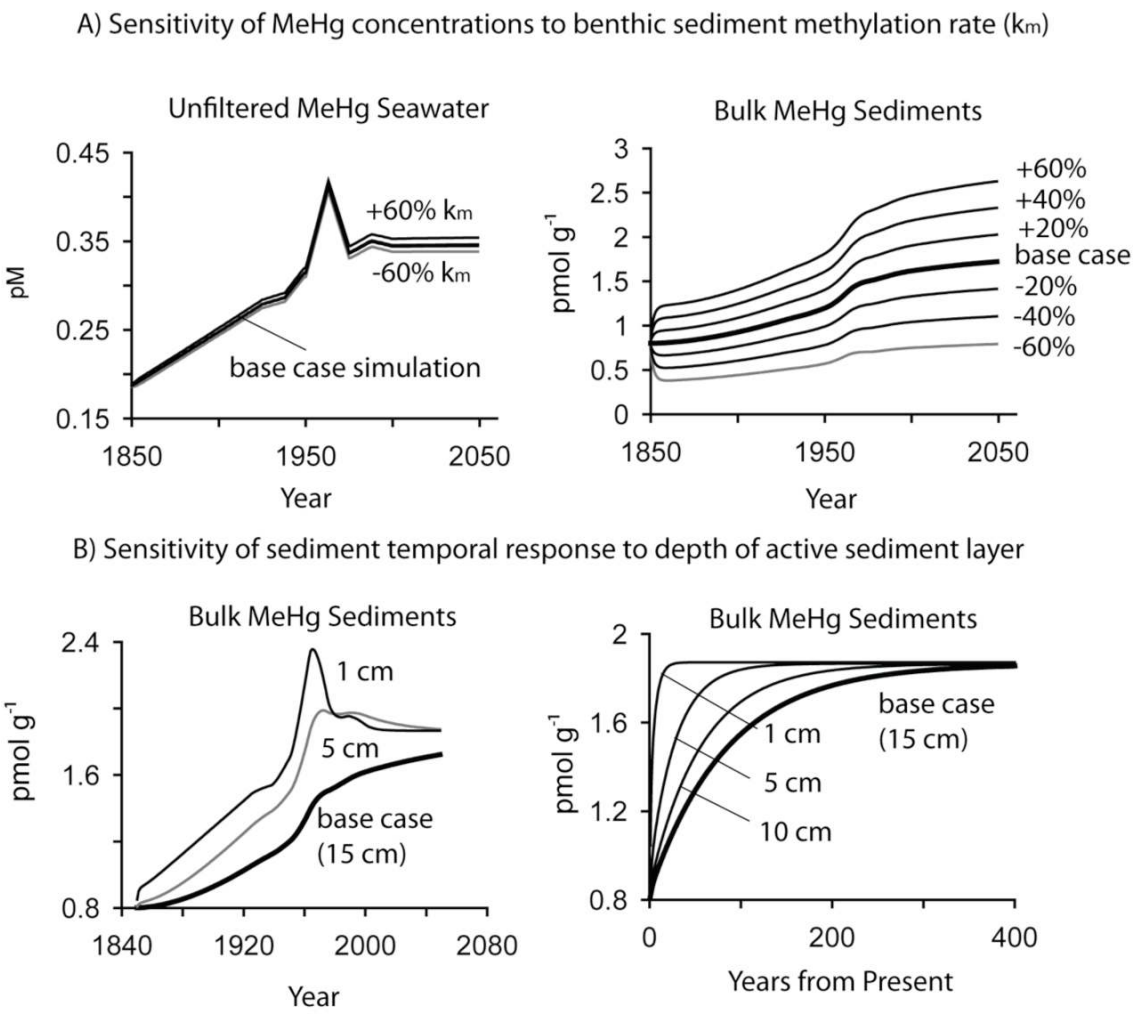

Figure S2. Selected model sensitivity analysis results. Panel (A) shows changes in sediment and water column MeHg concentrations with benthic sediment methylation rate changes. Panel (B) shows changes in the temporal response of benthic sediment MeHg concentrations with changes in the active sediment layer depth. Left panel shows historical simulation, while right panel shows changes in concentrations for 400 years simulated by forcing the model with present-day (ca. 2000) loadings.

Table S1. Sensitivity analysis of change in year 2000 seawater (C_w) MeHg concentrations with changes in the sediment methylation rate (k_m), and reduction rate (k_{red})

C_w MeHg	-60%	-40%	-20%	+20%	+40%	+60%
k_m	-2.14%	-1.45%	-0.72%	+0.69%	+1.39%	+2.08%
k_{red}	0.58%	0.35%	0.17%	-0.17%	-0.32%	-0.43%

Section I: Site-specific data

Table S2. Measured Hg concentration data.

Description	Mercury concentrations (mean±stdev)	
	Total Hg	MeHg
Benthic sediments		
Bulk sediments (pmol/g)	209±65	1.50±0.45
Interstitial water (pM)	70±33	4.4±2.5
Partition coefficient (log K_D, L/kg)	3.56±0.19	2.57±0.27
Potential methylation rate (d^{-1})	n/a	0.0264
Seawater (pM)		
June 2001 (n=10)	1.52±0.62	0.19±0.09
Nov. 2001 (n=4)	1.07±0.18	0.32±0.08
Aug. 2002 (n=8)	1.22±0.22	0.25±0.10
Partition coefficient (log K_P, L/kg)	5.61 (Hg(II))	4.35
Tidal Inflow (pM)		
Aug. 2000 (n=17)	1.21±0.29	n/a
June 2001 (n=29)	1.28±0.49	0.26±0.12
Aug. 2002 (n=26)	1.10±0.25	0.32±0.11
Atmospheric data		
[a]Total gaseous Hg (pmol m^{-3})	7.08	n/a
[a]Average wet deposition (nmol m^{-2} yr^{-1})	30.9±6.7	n/a
Total annual deposition (nmol m^{-2} yr^{-1})	54.8±0.5	0.50±0.35[b]
Rivers (pM)		
Magaguadavic (Nov.)	18.8±13.9	1.36
Magaguadavic (May)	22.1±4.0	1.58
Magaguadavic (Aug.)	8.7±3.9	n/a
Digdegaush (Nov.)	25.4±11.1	1.35
Digdegaush (May)	29.1±4.1	1.27
Digdegaush (Aug.)	7.8±3.0	n/a
St. Croix (Nov.)	20.2	0.68
St. Croix (May)	21.0±1.0	1.39
St. Croix (Aug.)	10.6±4.9	n/a

n/a = not available. Benthic sediment data are from Sunderland et al. *(1, 2)*. Seawater and river data are from Dalziel et al. *(3, 4)*. Partition coefficient for seawater is based on measured concentrations in phytoplankton *(5)*. Atmospheric data are from the Mercury Deposition Network (MDN) station NB-02 in St. Andrews, New Brunswick (45.0833N, 67.0833W) *(6, 7)*, Sunderland et al. *(8)*, and data from Environment Canada.

Seawater collection and analysis methods:

Sampling sites in Passamaquoddy Bay and the outer Bay of Fundy representative of tidal waters flowing into Passamaquoddy Bay were occupied on three expeditions from 2000 to 2002. The site locations were selected to sample the Scotian Shelf inflow to the Bay of Fundy and the deep-water inflow from Northeast Channel. Unfiltered water samples for both total and methyl mercury were collected using a General Oceanics Lever Action Niskin® modified for trace metal sampling. The Niskin modification involved Teflon - end caps, drain spout and internal coating. To further reduce the possibility of contamination, established clean sampling methods were employed *(9)*. Sub-sampling was carried out in a clean area of boat and the water collected for Hg drawn first from the Niskin. The water samples were collected into a precleaned Teflon bottles and double bagged until the samples could be preserved. Samples were preserved with 2 ml L^{-1} BrCl (total Hg) and 2 ml L^{-1} 9M H_2SO_4 (MeHg) within 2 hours of collection when the boat became stable or at dockside. All samples were analyzed in a dedicated mercury laboratory using EPA Methods 1631 for total Hg and 1630 for methyl Hg. For total Hg analysis, samples were digested at 60°C for 24 hours and if excess BrCl was not evident in the sample, additional BrCl was added and the heat-digestion step repeated. Methyl Hg samples were stored at -4 °C prior to analysis. Further Methods and detection limits (total Hg: 0.20 pM; MeHg 32 fM) for Passamaquoddy Bay samples were those described in Sunderland et al. *(1)* for aqueous samples.

Table S3. Summary of study-site characteristics.

Physical/Biological Properties	
Water surface area (m^2)	1.32×10^8
Sediment surface area (m^2)	1.48×10^8
Intertidal surface area (m^2)	1.54×10^7
Water volume (m^3)	2.81×10^9
Active sediment layer depth (m)	0.015
Sediment volume (m^3)	2.22×10^9
Average wind speed (m s^{-1}) (7 m above surface)	4.56±1.14
Average water depth (m)	30 m
Average water temperature (°C)	9
Average salinity (‰)	30
Net primary productivity (g C m^{-2} yr^{-1})	296
Average shortwave radiation intensity (W m^{-2})	211
Average daylight hours (St. Andrews, NB)	12.21
Shortwave radiation adj. for cloud cover and daylight (W m^{-2})	70
Hydrologic Properties	
Seawater outflow (m^3 yr^{-1})	6.41×10^{10}
Precipitation inputs (average 1996-2004, m^3 yr^{-1})	1.41×10^8
Freshwater inflow into estuary (m^3 yr^{-1})	4.68×10^9
Flushing time (days)	16
Tidal inflow (m^3 yr^{-1})	5.92×10^{10}
Solids Characteristics	
Water column suspended solids concentration (kg L^{-1})	1.76×10^{-6}
Suspended solids density (kg L^{-1})	1.5
Organic carbon content of suspended solids (unitless)	0.14±0.05
Median suspended solids particle diameter (μm)	5.0
Solids concentration in benthic sediment (kg L^{-1})	0.67
Benthic sediment solids density (kg L^{-1})	2.65
Tidal waters suspended solids concentration (kg L^{-1})	3.67×10^{-6}
Freshwater inflow suspended solids concentration (kg L^{-1})	3.40×10^{-6}
Benthic sediments organic carbon content (unitless)	0.018±0.006
Basin-wide average burial rate of benthic sediments (cm yr^{-1})	0.082
Intertidal sediment burial rate (cm yr^{-1})	0.55 (0.37-0.65)
Intertidal sediment bulk density (kg L^{-1})	0.57 (0.49-0.64)

Physical data from: Gregory et al. *(10)*, Sunderland et al. *(2)*, Robinson et al. *(11)*, and (GoMOOS JO2: http://www.gomoos.org/gnd); *Hydrologic* data from: Gregory et al. *(10)* and Ketchum and Kern *(12)* and average precipitation rate (1.065 m yr^{-1}) measured at St. Andrews, NB (45.09°N 67.00°W) between 1996-2004 *(6, 7)*; *Solids balance* data from: Sunderland et al. *(1, 2)*, Showell and Gaskin *(13)*, Dalziel et al. *(3, 4)*, Gobas et al. *(14)* and Hung and Chmura *(15)*.

Section II: Differential equation for total Hg, Hg(0), Hg(II), and MeHg

Total Mercury

For total Hg, the model simulates time-dependent (t) changes in the water (M_w, mol) and sediments (M_s, mol) reservoirs as follows:

$$\frac{dM_w}{dt} = (A + R + T) + (k_{res} + k_{diff})M_s - (k_{ev} + k_o + k_{sett})M_w$$

$$\frac{dM_s}{dt} = k_{sett}M_w - (k_{res} + k_{bur} + k_{diff})M_s$$

Where,

A = atmospheric deposition (mol d^{-1})
R = river discharges (mol d^{-1})
T = tidal inflow (mol d^{-1})
k_{res} = rate coefficient for benthic solids resuspension (d^{-1})
k_{diff} = rate coefficient for sediment-to-water diffusion of Hg(II) and MeHg (d^{-1})
k_{ev} = rate coefficient for evasion of Hg(0) from the water column (d^{-1})
k_o = rate coefficient for seawater outflow (d^{-1})
k_{sett} = rate coefficient for settling of suspended particles (d^{-1})
k_{bur} = rate coefficient for burial of benthic solids (d^{-1})

Hereon, for each major form of Hg, we denote total external loading of dissolved and particulate phase Hg as "*L*" (mol d^{-1}).

Methylmercury (MeHg)

Water column:

$$\frac{dM_{wMeHg}}{dt} = L_{MeHg} + (k_{res(MeHg)} + k_{diff(MeHg)})M_{sMeHg} - (k_{o(MeHg)} + k_{sett(MeHg)} + k_{dmw})M_{wMeHg}$$

Benthic sediments:

$$\frac{dM_{sMeHg}}{dt} = k_{sett(MeHg)}M_{wMeHg} - (k_{res(MeHg)} + k_{bur(MeHg)} + k_{diff(MeHg)})M_{sMeHg} - k_{dm}M_{sdMeHg} + k_m M_{sdHgII}$$

Where,

k_m = rate coefficient for methylation (d^{-1})
k_{dm} = rate coefficient for demethylation (d^{-1})
M_{sd} = dissolved reservoir of Hg in benthic sediments, used as a proxy for the bioavailable pools for methylation and demethylation. The dissolved pool is calculated at each time step in the simulation based on empirically measured partition coefficients (K_d) for MeHg and Hg(II) *(1, 2)*.

Elemental Mercury (Hg(0))

Water column:

$$\frac{dM_{wHg0}}{dt} = L_{Hg0} + k_{red}\phi M_{wHgII} - (k_{o(Hg0)} + k_{ev(Hg0)} + k_{ox})M_{wHg0}$$

Where,

k_{ox} = rate coefficient for oxidation of Hg(0) in the water column. We include terms for both photo-oxidation *(16)* and dark oxidation *(17, 18)* in the overall oxidation rate.

k_{red} = rate coefficient for reduction of Hg(II) in the water. Terms for photolytic and biotic reduction *(16, 19)* are included in the overall reduction rate.

ϕ = fraction of Hg(II) in the water column that is reducible.

Benthic sediments:

We do not include Hg(0) in benthic sediments because there are no data on Hg(0) concentrations in marine sediments.

Divalent mercury (Hg(II))

Water column:

$$\frac{dM_{wHgII}}{dt} = L_{HgII} + (k_{sw(HgII)} + k_{diff(HgII)})M_{sHgII} - (k_{o(HgII)} + k_{ws(HgII)} + k_{red})M_{wHgII}$$
$$+k_{dm}M_{sdMeHg} + k_{dmw}M_{wMeHg} + k_{ox}M_{wHg(0)}$$

Benthic sediments:

$$\frac{dM_{sHgII}}{dt} = k_{ws(HgII)}M_{wHgII} - (k_{sw(HgII)} + k_{diff(HgII)} + k_{b(HgII)})M_{sHgII} + k_m M_{sdHgII} + k_{dm}M_{sdMeHg}$$

Section III: External loading from rivers, tides and atmospheric deposition

Rivers

Table S4. Cumulative freshwater discharges (m^3 mo^{-1} x 10^8) into Passamaquoddy Bay reported by Gregory et al. *(10)*.

Winter			*Spring*			*Summer*			*Fall*		
Jan	Feb	Mar	Apr	May	Jun	Jul	Aug	Sept	Oct	Nov	Dec
3.34	3.03	4.32	8.82	6.37	3.51	2.54	2.21	2.06	2.78	3.68	4.12
Percent discharge by season:											
22.9%			40.0%			14.5%			22.6%		

The three major freshwater tributaries flowing into Passamaquoddy Bay are the Digdegaush (13.1%), Magaguadavic (25.2%) and St. Croix Rivers (61.7%) *(20)*. Solids and dissolved phase inputs were determined based on the suspended solids concentrations and partition coefficients for Hg(II) and MeHg derived from the particulate organic carbon content of suspended solids *(13)*. Concentrations of suspended particulate matter measured in freshwater discharges ranged between 1.19 and 6.19 mg $L^{-1}$with a weighted annual average concentration of suspended particulates of 3.43±1.03 mg L^{-1}

Historical Loading

We calculate historical loading by applying anthropogenic enrichment factors (AEFs) from sediment records (for atmospheric and fluvial inputs) *(2, 8)* and a linear extrapolation of anthropogenic enrichment modeled in the North Atlantic Ocean *(21)*. We divide measured inputs (ca. 2000) by the AEF for 1850 and then extrapolate results to intermediate years using the AEF corresponding to each year. We calculate upper and lower 95% confidence intervals for loading based on the measured variability in year 2000 inputs. We interpolate between years assuming a linear rate of change in loading.

Speciation

Table S5. Speciation of loading from tides, rivers and atmospheric deposition. For all simulations, speciation of Hg in inputs assumed to be constant based on measured concentrations of total Hg and MeHg. High, mean and low estimates are based on variability in the measured data.

	MeHg	Hg(0)	Hg(II)
	Atmospheric deposition		
Mean	0.9%	n/a	99.1%
Low 95% CI	0.2%	n/a	99.8%
High 95% CI	1.4%	n/a	98.6%
	Fluvial inputs		
Mean	6.5%	10.0%	83.6%
Low 95% CI	5.6%	10.0%	84.4%
High 95% CI	8.6%	10.0%	81.4%
	Tidal inputs		
Mean	24.3%	13.0%	62.8%
Low 95% CI	20.7%	7.0%	72.3%
High 95% CI	26.3%	19.0%	54.7%

n/a = not applicable. Net flux of Hg(0) is modeled explicitly in the derivation of the evasion rate coefficient (see section IV). Based on Amyot et al. *(22)*, we assume that Hg(0) is 10% of the total loading.

Section IV: Derivation of model rate coefficients

Table S6. Summary of model rate coefficients for year 2000 simulation (d^{-1}). Descriptions of methods and data used to derive each rate constant are provided below.

Process	Rate Coefficients
Seawater outflow	$k_o = 0.0625$
Evasion of Hg(0)	$k_{ev} = 0.0490$
Solids settling Hg(II)	$k_{sett} = 0.0402$
Solids resuspension Hg(II)	$k_{res} = 9.74 \times 10^{-6}$
Burial Hg(II)	$k_{bur} = 2.38 \times 10^{-5}$
Sediment-to-water diffusion Hg(II)	$k_{diff} = 1.55 \times 10^{-6} – 7.33 \times 10^{-6}$
Benthic sediment methylation	$k_m = 0.0264$
Benthic sediment demethylation	$k_{dm} = 0.34$
Solids settling MeHg	$k_{sett(MeHg)} = 0.0036$
Photodecomposition of MeHg in water	$k_{dmw} = 0.0015$
Solids resuspension MeHg	$k_{res} = 9.70 \times 10^{-6}$
Burial MeHg	$k_{bur(MeHg)} = 2.37 \times 10^{-5}$
Sediment-to-water diffusion MeHg	$k_{diff(MeHg)} = 1.55 \times 10^{-5} – 9.14 \times 10^{-5}$
Photo-oxidation of Hg(0) in water	$k_{ox1} = 0.6081$
Photo-reduction of Hg(II) in water	$k_{red1} = 0.6408$
Dark oxidation of Hg(0) in water	$k_{ox2} = 0.4840$
Biotic reduction of Hg(II) in water	$k_{red2} = 0.0287$

Sediment burial

Benthic sediment burial rates were measured using vertical gradients of dissolved ammonium and sulfate in gravity cores collected at multiple stations (n=20) following the method developed by Cranston *(23, 24)*. Details of sampling and analytical techniques are reported in Sunderland et al. *(2)*. The intertidal area was calculated from the difference between water surface area at low and high tide from Gregory et al. *(10)* and accounts for 10% of the total sediment surface area in the Bay.

The coefficient for sediment burial (k_b) is based on burial rates measured in gravity cores collected at multiple stations (n=27) *(2)*. For the main bay, we constructed a spatial grid of sediment accumulation using Kriging as a spatial interpolation method and estimated annual sediment burial across the system by summing volume estimates for each cell defined in the spatial grid (see burial flux diagram Figure 1). We also include sediment burial in intertidal mudflats based on measured Hg concentrations and accumulation rates reported in Hung and Chmura *(15)*. The total burial flux is the sum of burial in intertidal areas and the main bay. We divide this total flux by the surface area of the sediments to calculate an average basin wide burial rate (v_b, m d^{-1}), which we assume to be constant between 1850 and 2050. Rate coefficients for sediment burial of Hg(II) and MeHg (k_b, d^{-1}) are calculated from v_b, the sediment surface area (SA_{sed}, m^2), the sediment volume (V_{sed}, m^3), and the fraction of Hg(II) or MeHg in the dissolved phase of benthic sediments, as follows:

$$k_{bur} = SA_{sed} \bullet v_b \bullet (1 - f_{diss(sed)}) / V_{sed}$$

The $f_{diss(sed)}$ is based on the empirically measured partition coefficients for Hg(II) and MeHg in benthic sediments (K_D, L kg^{-1}, Table S2) and the concentrations of solids in benthic sediments (C_{ss}, kg L^{-1}):

$$f_{diss(sed)} = \frac{1}{(1 + K_D C_{SS})}$$

Settling of suspended solids

Rate coefficients for settling ($k_{ws,}$ d^{-1}) of Hg(II) and MeHg are based on the particle settling velocity (v_s, m d^{-1}), water surface area (SA_W, m^2), water volume ($V_{w,}$ m^3), and the fraction of dissolved Hg(II) or MeHg in the water column (f_{diss}, dimensionless):

$$k_{sett} = SA_W \bullet v_s \bullet (1 - f_{diss}) / V_w$$

where f_{diss} is the calculated from the empirically measured particle-water partition coefficient (K_P, L kg^{-1}) and the concentration of suspended solids in the water column (SPM, kg L^{-1}):

$$f_{diss} = \frac{1}{(1 + K_P SPM)}$$

Particle size spectra of nepheloid layer sediments were measured by the Particle Dynamics Laboratory at the Bedford Institute of Oceanography using Coulter analysis *(25)* at 24 stations in Passamaquoddy Bay in August 2000. Median particle diameter was determined to be 5 μm based on this analysis, which we use to calculate the average settling velocity of particles.

We calculate the average settling velocity for particles (v_s) based on the measured mean particle diameter and Stoke's law for particles falling in a viscous fluid *(26)*:

$$v_s = \frac{2}{9} \frac{(d_{pw} - d_{sw})}{\mu} g r_{pw}^{\ 2}$$

v_s = settling velocity of suspended solids (m s^{-1})
d_{pw} = density of suspended particles in seawater (kg m^{-3})
d_{sw} = density of seawater (kg m^{-3})
μ = dynamic viscosity of seawater (Pa s^{-1})
g = gravitational acceleration (m s^{-2})
r_{pw} = average radius of suspended solids (m)

Figure S3. Summary of particle size distributions

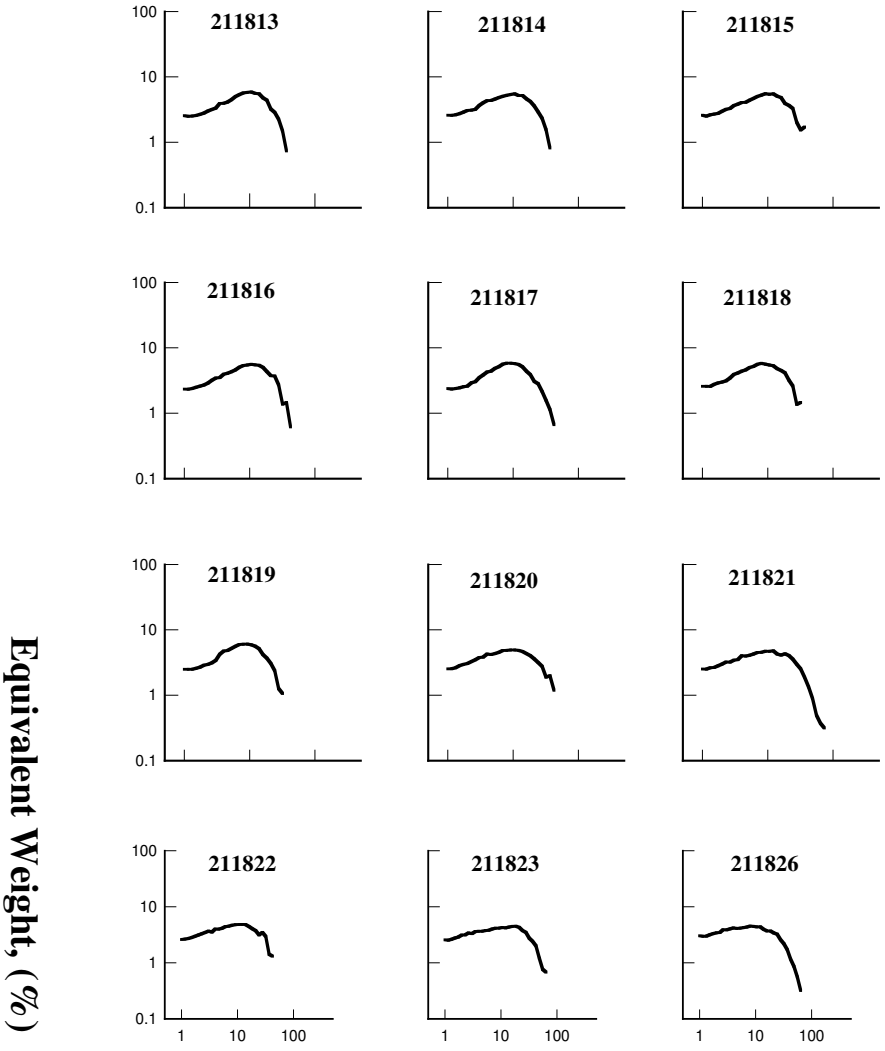

Particle Dynamics Lab, BIO

Solids resuspension

Rate coefficents for resuspension (k_{sw}, d^{-1}) of Hg(II) and MeHg are calculated as follows:

$$k_{res} = \mathrm{Re}\, sFlux / C_{ss} \bullet (1 - f_{diss(sed)}) / 1000 V_{sed}$$

where we assume that the solids resuspension flux (*ResFlux*) is equal to the difference between the settling and burial fluxes of solids (kg) *(14)*.

Sediment-to-water diffusion

Rate coefficients for diffusive fluxes of Hg(II) and MeHg from sediments into the water are calculated by dividing fluxes by the respective reservoirs of Hg species at each time step in the model simulation. Diffusional fluxes (*F*) of total Hg and MeHg are based on the parameterization described in Gill et al. *(27)* and Hammerschmidt et al. *(28)* and Fick's first law:

$$F = -\left(\frac{\varphi D_w}{\theta^2}\right)\frac{dC}{dx}$$

where F is the flux of solute (pmol m^{-2} d^{-1}); dC is the maximum concentration gradient of Hg species between depths (dx) and is assumed to be in the top 1 cm of the sediments; φ is the measured sediment porosity (0.74); θ is tortuosity ($1-\ln(\varphi^2)$); and D_w is the diffusion coefficient of the solute in water.

We model high and low ranges of diffusional fluxes for Hg(II) and MeHg using diffusion coefficients (cm^2 s^{-1}) calculated for different Hg species-complexes in sediment pore waters at 25°C. To calculate a lower bound for both Hg(II) and MeHg diffusion, we use a diffusion coefficient of $D_w = 2.0 \times 10^{-6}$, which was derived for macromolecular organic matter in the colloidal size range *(27)*. As an upper bound, we use diffusion coefficients of $D_w = 1.2 \times 10^{-5}$ *(28)* for MeHg and $D_w = 9.5 \times 10^{-6}$ *(27)* for Hg(II) based on CH_3HgSH^0 and $HgCl_4^{2-}$, respectively. Although other studies have suggested these species may not be the dominant complexes in porewaters, diffusion coefficients vary at most by a factor of two (T. Hollweg, UConn., PhD thesis) and thus the values for D_w chosen here are suitable for bounding high and low extremes of potential fluxes.

We calculate a temperature corrected diffusion coefficient based on the annual average water temperature of Passamaquoddy Bay (Table S3):

$$D_{w(T)} = D_{w(25)}/(1 + 0.048 \bullet (25 - T))$$

Methylation and demethylation rates

Methylation rate coefficients are based on measurements in sediment cores spiked with stable Hg(II) isotopes *(2, 29)* (Table S2). A detailed description of the experimental design and rate calculations can be found in Heyes et al. *(29)*. This method assumes that the added isotope is representative of the bioavailable pool of Hg(II), and that substantial depletion did not occur during the assay period. Spike concentrations were kept low (10-20% of in situ concentrations) to minimize the potential increase in Hg bioavailability with Hg(II) addition. Heyes et al. *(29)* showed across several estuaries that MeHg concentration is a good predictor of net methylation activity and that changes in MeHg concentrations are driven more by differences in the methylation rate than the demethylation rate. Heyes et al. *(29)* further hypothesized that the MeHg demethylation experiments actually underestimate MeHg demethylation compared to ratios Hg to MeHg concentrations in field samples, because a) the assumption of the back reaction of methylation is unimportant was not valid or b) some of the added MeHg becomes unavailable for demethylation over time. We also hypothesized that methylation and demethylation likely occur in similar zones of microbial activity thus newly methylated Hg maybe the most available for demethylation.

We therefore calibrated the demethylation rate to ensure that the ratio of methylation to demethylation matched the seasonally averaged measured percent MeHg in interstitial water. The fraction of total Hg present as MeHg in estuarine sediments has been shown to be a reliable indicator of net methylation in a variety of studies *(2, 28, 29)*. We use the dissolved pools of Hg(II) and MeHg in sediment pore waters as the bioavailable pool subject to microbial processes resulting in methylation and demethylation *(30)*.

We do not include *in situ* water column methylation because this system does not have the low oxygen conditions required to support net methylation *(32, 33)*.

Seawater outflow

The rate coefficient for seawater outflow (d^{-1}) of all species is the ratio of seaward flow to the estuarine volume and is based on the tidal flushing rate and the associated annually averaged daily net translocation of tidal water *(12)*. Ketchum and Keen *(12)* estimated the flushing time to be 16 days based on salinity measurements and freshwater inputs. The net volume of seaward flow (T_o) is estimated from this flushing time, which represents the length of time required for the estuary to exchange its volume (i.e., V_w/T_o = flushing time; where, V_w represents the average water volume of the estuary).

Photodecomposition of water column MeHg

The photodecomposition rate of MeHg in the water column is parameterized based on average shortwave radiation penetration in the water column (*RAD*, W m^{-2}), using data from Sellers et al. *(31)* ($k_{dmw} = 8.52 \times 10^{-4}$ x RAD). This relationship was derived in freshwater environments and is therefore highly uncertain when applied to marine seawater. However, bounding of photodecomposition based on the rate information provided in Sellers et al. *(31)* suggests that photodecomposition is a negligible component of water column MeHg losses on an annual basis (see Figure 2 main text). Methods and data used to calculate light attenuation in the water column are provided in Tables S3 and S7.

Oxidation and reduction rates

To characterize inorganic Hg redox reactions in the water column, we use dual isotope addition data from Whalin et al. *(16),* who confirmed that Hg oxidation (k_{ox}) and reduction (k_{red}) reactions occur simultaneously in seawater. We parameterize photo- reduction and oxidation as a function of total shortwave radiation and biotic reduction as a function of net primary productivity. By least-squares fit to rates reported in Whalin et al. *(16)*, we derived relationships between photoreduction, photoxidation and total shortwave radiation. Similarly, we derived from these data a relationship between the biotic reduction rate and productivity using values for the outer and shelf region of Chesapeake Bay characteristic of the measurement period *(34)*. We assume that the reducible pool of water column Hg(II) is 50% based on data showing colloidally bound species can account for >50% of Hg(II) in coastal waters and chloride complexes in marine waters may be more resistant to reduction *(16, 35)*.

We calculated an average light intensity throughout the water column of Passamaquoddy Bay using the local shortwave radiation flux and light attenuation based on spectral light absorption/scattering coefficients for seawater, DOC and pigments, and their respective

concentrations. Spectral light absorption coefficients listed below are from from the EXAMS model (see: http://www.epa.gov/ceampubl/swater/exams/index.html). We also include dark oxidation of Hg(0) based on Lalonde et al. *(17, 18)*.

Table S7. Summary of model parameters used to calculate oxidation of Hg(0) and reduction of Hg(II) in the water column.

Parameter	Description	Formulation
k_{ox1} (d^{-1})	photo-oxidation rate constant	$0.354 \bullet RAD$ *(16)*
k_{ox2} (d^{-1})	dark oxidation rate constant	0.484 *(17, 18)*
k_{red1} (s^{-1})	photolytic reduction rate constant	$0.373 \bullet RAD$ *(16)*
k_{bio} (s^{-1})	biotic reduction rate constant	$3.54 \times 10^{-2} \bullet NPP$ *(16)*
RAD_i (W m^{-2})	total local shortwave radiation penetration in the mixed layer	$\frac{1}{x_2 - x_1} \bullet \frac{RAD}{\eta}[e^{\eta x1} - e^{-\eta x2}]$
RAD (W m^{-2})	average annual shortwave radiation at the water surface	70
x_1 (m)	surface depth	0 m
x_2 (m)	average water depth	30 m
η (m^{-1})	extinction coefficient for radiation	$\eta_{water} + \eta_{Chl} C_{Chl} + \eta_{DOC} C_{DOC}$
η_{water} (m^{-1})	extinction coefficient for water	0.0145 (450 nm)
η_{Chla} (m^{-1})	extinction coefficient for pigments	31 (450 nm)
C_{Chla} (mg L^{-1})	average concentration of Chl a in mixed layer	0.65 x 10^{-3} *(13)*
η_{DOC} (mg L^{-1})	extinction coefficient for dissolved organic carbon (DOC)	0.654 (450 nm)
C_{DOC} (mg L^{-1})	average DOC concentrations in water column	2.0 *(36)*
NPP (gC m^{-2} d^{-1})	average annual net primary productivity	0.81 *(36)*

Evasion of Hg(0)

We model air-sea exchange of Hg(0) using the evasion scheme developed by Nightingale et al. *(37)* (referred to as 'N00' in Table S8) and wind speed data from a nearby (44°53'21" N, 67°00'44"W) Gulf of Maine Ocean Observing Station (GoMOOS JO2: http://www.gomoos.org/gnd). We compared this evasion flux to the scheme developed by Liss and Merlivat *(38)* (L&M86).

Total gaseous atmospheric Hg data are from MDN measurements in St. Andrews, NB *(6, 7)*, and water column Hg(0) concentrations are based on redox reaction rates. We use the temperature corrected Henry's Law constant for Hg(0) in seawater *(39)*, a temperature corrected Schmidt number for CO_2 *(40)*, and the temperature and salinity specific kinematic viscosity and diffusivity for Hg(0) calculated using the Wilke-Chang method *(41)*.

Table S8. Summary of parameters used to calculate air-sea exchange of Hg(0)

Parameter	Description	Formulation
F_v (nmol m^{-2} d^{-1})	Hg(0) air-sea exchange flux	$F_v = K_w(C_w - C_a / H'(T))$
C_w (pM)	concentration of Hg(0) in seawater	See differential equations
C_a (ng m^{-3})	concentration of Hg(0) in air	Mean MDN data NB-02 (Table S2)
H'(T)	Temperature dependent dimensionless Henry's law constant from Andersson et al. *(39)*	$\ln H' = (\frac{-2403.3}{T} + 6.92)$
T′ (ºC)	average water temperature	9 *(11)*
T (K)	water temperature in Kelvin	273 + T′
K_w (cm hr^{-1}) (N00)	water-side mass transfer coefficient for steady winds	$0.25u_{10}^2(Sc/Sc_{CO_2})^{-0.5}$
K_w (m s^{-1}) (L&M 86)	water-side mass transfer coefficient	For u_{10} >3.6 <13: $2.8\times10^{-6} \bullet (5.9u_{10} - 49.3) \bullet (Sc/Sc_{CO_2})^{-0.5}$
u_{10} (m s^{-1})	wind speed normalized to 10 m above sea surface, where z = measurement height (7m) and u_z = wind speed at measurement height.	$u_{10} = \frac{10.4u_z}{\ln(z) + 8.1}$
Sc_{CO_2}	Schmidt number for CO_2	$0.11T'^2 - 6.16T' + 644.7$ *(40)*
$Sc_{Hg(0)}$	Schmidt number for Hg(0)	ν / D
ν (cm^2 s^{-1})	kinematic viscosity	N/ρ = $0.017e^{(-0.025T')}$ *(40)*
N (cP)	viscosity of water	$1.88\times10^{-3} - 0.04\times10^{-3}T'$
ρ (mg cm^{-3})	seawater density	1025
D (cm^2 s^{-1})	diffusivity (Wilke-Chang *(41)* method)	$\frac{7.4\times10^{-8}(\phi_w M_w)^{1/2}T}{\mathrm{N}V_B^{0.6}}$
M_w (g mol^{-1})	molecular weight of water	18.0
V_B (cm^3 mol^{-1})	molal volume of mercury at its normal boiling temperature	12.74 *(42)*
ϕ_w	solvent association factor	2.26 *(43)*

References

(1) Sunderland, E. M.; Gobas, F. A. P. C.; Branfireun, B. A.; Heyes, A., Environmental controls on the speciation and distribution of mercury in coastal sediments. *Mar. Chem.* **2006,** *102*, 111-123.

(2) Sunderland, E. M.; Gobas, F. A. P. C.; Heyes, A.; Branfireun, B. A.; Bayer, A. K.; Cranston, R. E.; Parsons, M. B., Speciation and bioavailability of mercury in well-mixed estuarine sediments. *Mar. Chem.* **2004,** *90*, 91-105.

(3) Dalzeil, J. A.; Yeats, P. A.; Amirault, B. P., Inorganic chemical analysis of major rivers flowing into the Bay of Fundy, Scotian Schelf, and Bras d'Or Lakes. *Canadian Technical Report of Fisheries and Aquatic Sciences* **1998,** *2226*, (vii), 140.

(4) Dalziel, J.; Harding, G.; Sunderland, E., The mercury flux of an east coast marine embayment. In *8th International Conference on Mercury as a Global Pollutant*, Madison, WI, USA, 2006.

(5) Harding, G.; Dalziel, J.; Vass, P. In *Prevalence and bioaccumulaton of methylmercury in the food web of the Bay of Fundy, Gulf of Maine*, 6th Bay of Fundy Workshop, Cornwallis, Nova Scotia, Canada, September 29–2 October 2004, 2004; Percy, J. A., Evans AJ, Wells PG, Rolston SJ, Ed. Environment Canada, Atlantic Region: Cornwallis, Nova Scotia, Canada, 2004; pp 76-77.

(6) Kellerhals, M., et al., Temporal and spatial variability of total gaseous mercury in Canada: results from the Canadian Atmospheric Mercury Measurement Network (CAMNet). *Atmos. Environ.* **2003,** *37*, 1003-1011.

(7) Temme, C.; Blanchard, P.; Steffen, A.; Banic, C.; Beauchamp, S.; Poissant, L.; Tordon, R.; Wiens, B., Trend, seasonal and multivariate analysis study of total gaseous mercury data from the Canadian atmospheric mercury measurement network (CAMNet). *Atmos. Environ.* **2007,** *41*, 5423-5441.

(8) Sunderland, E.; Cohen, M.; Selin, N.; Chmura, G., Reconciling models and measurements to assess trends in atmospheric mercury deposition. *Environ Poll* **2008,** *156*, 526-535.

(9) Gill, G.; Fitzgerald, W., Mercury in surface waters of the open ocean. *Global Biogeochem. Cy.* **1987,** *3*, 199-212.

(10) Gregory, D.; Petrie, B.; Jordan, F.; Langille, P., Oceanographic, geographic and hydrological parameters of Scotia-Fundy and southern Gulf of St. Lawrence inlets. *Canadian Technical Report of Hydrographic Ocean Sciences* **1993**, (143), 248.

(11) Robinson, S. M. C.; Martin, J. D.; Page, F. H.; Losier, R. *Temperature and Salinity Characteristics of Passamaquoddy Bay and Approaches Between 1990-1995*; Canadian Technical Report of Fisheries and Aquatic Sciences No. 2139: St. Andrews, N.B., 1996.

(12) Ketchum, B. H.; Keen, D. J., The exchange of fresh and salt waters in the Bay of Fundy and in Passamaquoddy Bay. *Journal of the Fisheries Research Board of Canada* **1953,** *10*, (3), 97-121.

(13) Showell, M. A.; Gaskin, D. E., Partitioning of cadmium and lead within seston of coastal marine waters of the western Bay of Fundy. *Archives of Environmental Contamination and Toxicology* **1992,** *22*, 322-333.

(14) Gobas, F. A. P. C.; Z'Graggen, M. N.; Zhang, X., Time response of the Lake Ontario ecosystem to virtual elimination of PCBs. *Environ Sci Technol* **1995,** *29*, (8), 2038-2046.

(15) Hung, G. A.; Chmura, G., Mercury accumulation in surface sediments of salt marshes in the Bay of Fundy. *Environ. Poll.* **2006,** *142*, 418-431.

(16) Whalin, L.; Kim, E.; Mason, R., Factors influencing the oxidation, reduction, methylation and demethylation of mercury species in coastal waters. *Mar. Chem.* **2007,** *107*, 278-294.

(17) Lalonde, J.; Amyot, M.; Kraepiel, A.; Morel, F., Photooxidation of Hg(0) in artificial and natural waters. *Environ. Sci. Technol.* **2001,** *35*, 1367-1372.
(18) Lalonde, J. D.; Amyot, M.; Orvoine, J.; Morel, F. M. M.; Auclair, J. C.; Ariya, P. A., Photoinduced oxidation of Hg-0 (aq) in the waters from the St. Lawrence estuary. *Environ. Sci. Technol.* **2004,** *38*, (2), 508-514.
(19) Rolfhus, K.; Fitzgerald, W. F., The evasion and spatial/temporal distribution of mercury species in Long Island Sound, CT-NY. *Geochim. Cosmochim. Ac.* **2001,** *65*, (3), 407-418.
(20) Pol, R. A. *Chemical Loadings (Exports) to the Bay of Fundy: A Framework for Concentrations and Exports from Atlantic Canada Rivers*; International Joint Commission: Windsor, ON, Canada, January 1996, 1996.
(21) Sunderland, E. M.; Mason, R., Human impacts on open ocean mercury concentrations. *Global Biogeochem. Cy.* **2007,** *21*, GB4022.
(22) Amyot, M.; Lean, D. R. S.; Poissant, L.; Doyon, M.-R., Distribution and transformation of elemental mercury in the St. Lawrence River and Lake Ontario. *Can. J. Fish. Aquat. Sci.* **2000,** *57 (Suppl. 1)*, 155-163.
(23) Cranston, R. E., Sedimentation rate estimates from sulfate and ammonia gradients. *Proceedings of the Ocean Drilling Program, Scientific Results* **1991,** *119*, 401-405.
(24) Cranston, R. E., Organic carbon burial rates across the Arctic Ocean from the 1994 Arctic Ocean Section expedition. *Deep Sea Research II* **1997,** *44*, (8), 1705-1723.
(25) Loring, D. H.; Milligan, T. G.; Willis, D. E.; Saunders, K. S. *Metallic and Organic Contaminants in Sediments of the St. Croix Estuary and Passamaquoddy Bay*; Canadian Technical Report of Fisheries and Aquatic Sciences No. 2245: Dartmouth, N.S., 1998; p 38.
(26) Knightes, C., Development and test application of SERAFM: A screening-level mercury fate model and tool for evaluating wildlife exposure risk for surface waters with mercury-contaminated sediments. *Environmental Software and Modelling* **2008,** *23*, 495-510.
(27) Gill, G. A.; Bloom, N. S.; Cappellino, S.; Driscoll, C. T.; Dobbs, C.; McShea, L.; Mason, R.; Rudd, J. W. M., Sediment-water fluxes of mercury in Lavaca Bay, Texas. *Environ. Sci. Technol.* **1999,** *33*, (5), 663-669.
(28) Hammerschmidt, C.; Fitzgerald, W.; Lamborg, C.; Balcom, P.; Visscher, P., Biogeochemistry of methylmercury in sediments of Long Island Sound. *Mar. Chem.* **2004,** *90*, 31-52.
(29) Heyes, A.; Mason, R.; Kim, E.; Sunderland, E., Mercury methylation in estuaries: Insights from measuring rates using stable mercury isotopes. *Mar. Chem.* **2006,** *102*, 134-147.
(30) Benoit, J. M.; Gilmour, C. C.; Heyes, A.; Mason, R. P.; Miller, C., Geochemical and biological controls over methylmercury production and degradation in aquatic systems. *ACS Symp. Ser.* **2003,** *835*, 262-297.
(31) Sellers, P.; Kelly, C. A.; Rudd, J. W. M.; MacHutchon, A. R., Photodegradation of methylmercury in lakes. *Nature* **1996,** *380*, 694.
(32) Eckley, C. S.; Hintelmann, H., Determination of mercury methylation potentials in the water column of lakes across Canada *Sci. Tot. Environ.* **2006,** *368*, 111-125.
(33) Sunderland, E. M.; Krabbenhoft, D. P.; Moreau, J. W.; Strode, S. A.; Landing, W. M., Mercury sources, distribution, and bioavailability in the North Pacific Ocean: Insights from data and models. *Global Biogeochem. Cy.* **2009,** *23*, 14.
(34) Cerco, C., Phytoplankton kinetics in the Chesapeake Bay Eutrophication Model. *Water Quality and Ecosystem Modeling* **2000,** *1*, 5-49.
(35) Guentzel, J. L.; Landing, W. M.; Gill, G. A.; Pollman, C. D., Processes influencing rainfall deposition of mercury in Florida. *Environ. Sci. Technol.* **2001,** *35*, (5), 863-873.

(36) O'Reilly, J.; Evans-Zetlin, C.; Busch, D., Primary Production. In *Georges Bank*, Backus, R. H.; Bourne, D. W., Eds. MIT Press: Cambridge, MA, 1987; pp 220-233.
(37) Nightingale, P.; Malin, G.; Law, C.; AJ, W.; Liss, P.; Liddicoat, M.; Boutin, J.; Upstill-Goddard, R., In situ evaluation of air-sea gas exchange parameterizations using novel conservative and volatile tracers. *Global Biogeochem. Cy.* **2000,** *14*, (1), 373-387.
(38) Liss, P. S.; Merlivat, L., Air-sea exchange rates: Introduction and synthesis. In *The role of Air-Sea Exchange in Geochemical Cycling*, Buat-Menard, P., Ed. D Reidel Publishing Compant: Dodrecht, 1986; pp 113-127.
(39) Andersson, M. E.; Gardfeldt, K.; Wangberg, I.; Stromberg, D., Determination of Henry's law constant for elemental mercury. *Chemosphere* **2008,** *73*, (4), 587-592.
(40) Poissant, L.; Amyot, M.; Pilote, M.; Lean, D., Mercury water-air exchange over the upper St. Lawrence River and Lake Ontario. *Environ. Sci. Technol.* **2000,** *2000*, (34), 3069-3078.
(41) Wilke, C. R.; Chang, P., Correlation of diffusion coefficients in dilute solutions. *Aiche J.* **1955,** *1*, (2), 264-270.
(42) Loux, N. T., A critical assessment of elemental mercury air/water exchange parameters. *Chem. Speciation Bioavail.* **2004,** *16*, (4), 127-138.
(43) Hayduk, W.; Laudie, H., Prediction of diffusion-coefficients for nonelectrolytes in dilute aqueous solutions. *Aiche J.* **1974,** *20*, (3), 611-615.